CHEMISTRY OF MATERIALS

ARTICLE

pubs.acs.org/cm

Phalloidin-Functionalized Hyperbranched Conjugated Polyelectrolyte for Filamentous Actin Imaging in Living Hela Cells

Kai Li, Kan-Yi Pu, Liping Cai, and Bin Liu*

Department of Chemical and Biomolecular Engineering, 4 Engineering Drive 4, National University of Singapore, Singapore 117576, Singapore

Supporting Information

ABSTRACT: A phalloidin-functionalized hyperbranched conjugated polyelectrolyte (HCPE-phalloidin) is synthesized and used for direct filamentous actin (F-actin) imaging in living Hela cells. Different from commercially available organic dye-phalloidin conjugates, which require sophisticated techniques to be delivered into living cells, simple incubation of living cells with HCPE-phalloidin leads to efficient internalization of the probe and clear visualization of F-actin due to high brightness of HCPE and good specificity between phalloidin and actin. In addition, HCPE-phalloidin possesses improved photostability as compared to that for commercially available Alexa Fluor 488-phalloidin conjugates, suggesting that the new probe is promising for long-term F-actin imaging in living cells. Further fine-tuning the fluorescent property and targeting ability of HCPE-based probes could lead to more complicated imaging applications and subcellular target detection.

KEYWORDS: conjugated polyelectrolyte, hyperbranched conjugated polymer, nanospheres, fluorescence living cell imaging, F-actin, phalloidin

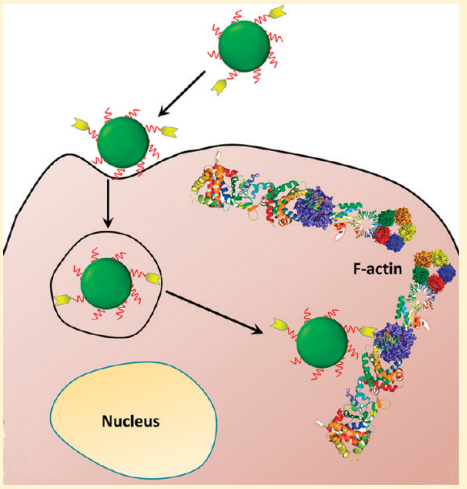

INTRODUCTION

Imaging and tracking cytoplasmic proteins in living cells through feasible and efficient fluorescent techniques remains a vital challenge in biological and biomedical research.[1−3] As an important protein in all eukaryotic cells, actin is implicated in a number of cellular activities, which include shape determination, cytokinesis, and cell motility.[4,5] Labeling actin in living cells offers great potentials for understanding the dynamics of various intracellular processes.[6−14] However, to achieve living cell imaging of actin, sophisticated techniques (e.g., microinjection, electroporation and permeabilization) or nanocarriers (e.g., liposomes) are required to deliver organic fluorophore or quantum dot (QD) conjugates into living cells due to inefficient living cell membrane permeability of these fluorescent species.[6−14] An alternative strategy relies on green fluorescent protein (GFP)-actin fusion proteins which can be integrated into actin filaments after delicate transfection.[15,16] These processes generally require multiple steps, which increase the imaging complexity and may alter the state of cells. In addition, intrinsic disadvantages of these fluorescent probes, such as poor photostability for organic fluorophores and GFP, and cytotoxicity for QDs, greatly restrict their applications in imaging living biosubstrates.[17] The development of novel fluorescent materials with high cellular internalization efficiency, good photostability, and high specificity for actin cytoskeleton staining is in urgent demand.

Conjugated polyelectrolytes (CPEs) are water-soluble conjugated polymers with highly delocalized backbone structures.[18,19] As compared to their small molecule counterparts, CPEs have larger absorption cross-sections and higher brightness.[20−22] Because of their good photostability and low cytotoxicity, there is increasing interest in using CPEs as nonspecific fluorescent probes for cellular imaging.[23−29] Although CPE-based selective recognition of extracellular matrix protein through nonspecific polyvalent interaction has been demonstrated,[24] subcellular protein targeting in living cells with specific CPEs remains a challenge. To achieve living cell intracellular protein detection, the CPE has to be designed with efficient intracellular delivery and specific targeting capability.[30−33] Motivated by the fact that three-dimensional dendrimers or nanoparticles with sizes of 20−50 nm could be efficiently internalized by living cells,[34−39] we look for conjugated polymers born with surface functional groups and three-dimensional structures. It occurs to us that hyperbranched conjugated polymers have been reported to show tunable optical properties, three-dimensional structures with flexible surface functionalization.[26,40−42] In addition, because of their intrinsic fluorescence, these polymers are significantly different from traditional dendrimers, which rely on dye conjugation

Received: December 14, 2010
Revised: March 15, 2011
Published: March 30, 2011

to yield fluorescence and share the drawback of dye molecules, such as photobleaching and low brightness.[43] As such, water-soluble hyperbranched CPEs could serve as a potential platform for construction of fluorescent probes for targeted biosubstrate imaging in living cells.

In this contribution, we report that the phalloidin-functionalized hyperbranched conjugated polyelectrolyte (HCPE-phalloidin) is suitable for direct filamentous actin (F-actin) imaging in living Hela cells. The molecular design is based on a cationic HCPE core and a poly(ethylene glycol) (PEG) out layer to ensure its biocompatibility and weak nonspecific interaction with biomolecules. Commercially available phalloidin, a cyclic peptide, is chosen as the targeting moiety because of its high affinity to F-actin cytoskeleton.[44,45] The human epithelial carcinoma cell line, Hela cell, is used in this study because it is one of the most commonly used cancer cell lines for F-actin imaging.[14,46−50] The performance of HCPE-phalloidin in living cell F-actin imaging has been evaluated, which is superior to commercially available fluorescent phalloidin conjugates in terms of imaging simplicity, living cell internalization and photostability.

EXPERIMENTAL SECTION

Materials. Amino-phalloidin (phalloidin amino-, tosylate) was purchased from Enzo Life Sciences. Cationic 3-(4,5-dimethylthiazol-2-yl)-2,5-diphenyl tetrazolium bromide (MTT), sucrose, genistein, *N*-(3-dimethylaminopropyl)-*N*′-ethylcarbodiimide hydrochloride (EDAC), *N*-hydroxysulfosuccinimide sodium salt (Sulfo-NHS), trimethylamine, and penicillin-streptomycin solution were purchased from Sigma-Aldrich. Fetal bovine serum (FBS), trypsin-EDTA solution, Alexa Fluor 594-phalloidin, and Alexa Fluor 488-phalloidin were purchased from Invitrogen (Life Technologies). 10× PBS buffer with pH 7.4 (ultrapure grade) was a commercial product of first BASE Singapore. Milli-Q water was supplied by Milli-Q Plus System (Millipore Corporation, Breford, USA). Dulbecco's Modified Eagle Medium (DMEM) medium was purchased from National University Medical Institutes (NUMI, Singapore). Hela cells were provided by American Type Culture Collection.

Characterization. NMR spectra were collected on Bruker Avance 500 (DRX 500, 500 MHz). UV−vis spectra were recorded on a Shimadzu UV-1700 spectrometer. The fluorescence spectra were measured using a Perkin-Elmer LS-55 equipped with a xenon lamp excitation source and a Hamamatsu (Japan) 928 PMT, using 90 degree angle detection for solution samples. High-resolution transmission electron microscopy (HR-TEM) images were obtained from a JEOL JEM-2010 transmission electron microscope with an accelerating voltage of 200 kV. Average particle size was determined by laser light scattering (LLS) with particle size analyzer (90 Plus, Brookhaven Instruments Co. USA) at a fixed angle of 90° at room temperature.

Cell Cultures. Hela cells were cultured (37 °C, 5% CO_2) in Dulbecco's Modified Eagle Medium (DMEM) medium containing 10% fetal bovine serum and 1% penicillin streptomycin. Before experiment, the cells were precultured until confluence was reached.

Synthesis of P0. A Schlenk tube charged with 4-(9,9′-bis(6-bromohexyl)-7-ethynylfluorenyl)-7-ethynylbenzothiadiazole (100 mg, 0.15 mmol) was degassed with three vacuum-nitrogen cycles. A solution of cyclopentadienylcobaltdicarbonyl ($CpCo(CO)_2$) in anhydrous toluene (1.5 mL, 0.01 M) was then added to the tube, and the system was further frozen, evacuated, and thawed three times to remove oxygen. The mixture was vigorously stirred at 65 °C under irradiation with a 200 W Hg lamp (operating at 100 V) placed close to the tube for 8 h. After the mixture was cooled to room temperature, it was dropped into methanol (100 mL) through a cotton filter. The precipitate was collected and redissolved in tetrahydrofuran (THF). The resultant solution was filtered through 0.22 μm filter, and poured into hexane to precipitate the product. After drying in vacuum at 40 °C, the neutral hyperbranched polymer precursor (**P0**) was obtained as light brown powders (65 mg, 65%). ^{1}H NMR (500 MHz, $CDCl_3$, δ ppm): 8.50−7.20 (m, 9 H), 3.67 (s, ∼0.6 H), 3.30 (br, 4 H), 2.0 (br, 4 H), 1.70 (br, 4 H), 1.42−1.06 (m, 8 H), 0.77 (br, 4 H). ^{13}C NMR (125 MHz, $CDCl_3$, δ ppm): 155.41, 154.34, 153.73, 153.06, 151.10, 150.97, 150.91, 150.08, 141.43, 140.50, 137.87, 134.02, 131.45, 129.04, 128.53, 128.23, 126.54, 125.30, 123.97, 120.68, 120.30, 119.98, 84.60, 83.30, 80.88, 77.92, 55.27, 40.10, 33.91, 32.64, 29.06, 27.77, 23.65.

Synthesis of P1. **P0** (50 mg) was dissolved in THF (10 mL), and trimethylamine (2 mL) was added dropwise to the solution at −78 °C. The mixture was stirred for 12 h, and then allowed to warm to room temperature. The precipitate was redissolved by the addition of methanol (8 mL). After the mixture was cooled to −78 °C, additional trimethylamine (2 mL) was added, and the mixture was stirred at room temperature for 24 h. After solvent removal, acetone was added to precipitate **P1** as light brown powders (55 mg, 95%). ^{1}H NMR (500 MHz, CD_3OD, δ ppm): 8.77−7.35 (m, 9 H), 3.63 (s, ∼0.6 H), 3.28 (br, 4 H), 3.05 (s, 18 H), 2.05 (br, 4 H), 1.58 (br, 4 H), 1.20 (br, 8 H), 0.77 (br, 4 H).

Synthesis of HCPE-COOH. **P1** (15 mg, 0.008 mmoL) and N_3−PEG-COOH (71 mg, 0.125 mmoL) were dissolved in DMF (5 mL). The mixture was degassed, and then *N,N,N′,N″,N‴*-pentamethyldiethylenetriamine (PMDETA, 6 mg, 0.04125 mmoL) and CuBr (5.9 mg, 0.04125 mmoL) were added. After reaction at 65 °C under nitrogen for 24 h, the mixture was cooled to room temperature and filtered through 0.22 μm syringe driven filter. The filtrate was precipitated into diethyl ether. The crude product was redissolved in water and further purified by dialysis against Milli-Q water using a 3.5 kDa molecular weight cutoff dialysis membrane for 5 days. After freeze-drying, HCPE-COOH (16 mg, 77%) was obtained as brown fibers. ^{1}H NMR (500 MHz, CD_3OD, δ ppm): 8.55−7.88 (m, ∼9.6 H), 4.00−3.37 (m, ∼23.0 H), 3.17−3.00 (m, 22 H), 2.28 (m, 4 H), 1.60 (br, 4H), 1.5−1.20 (m, 8 H), 0.9 (m, 4 H).

Synthesis of HCPE-Phalloidin. The conjugation of HCPE-COOH with amino-phalloidin was carried out through EDAC coupling reaction. In brief, 0.22 mL of HCPE-COOH (18 mg/mL) aqueous solution and 0.76 mL of amino-phalloidin (1 mg/mL, methanol) were mixed and diluted to a total volume of 4 mL in borate buffer (0.2 M, pH 8.5). EDAC and Sulfo-NHS were then added into the solution at a stoichiometric molar ratio of HCPE-COOH/EDAC/Sulfo-NHS = 1/5/5. The reaction was allowed to carry on for 3 h at room temperature with gentle mixing. The obtained product was dialyzed using a 500 Da molecular weight cutoff dialysis membrane against Milli-Q water for 1 day to eliminate the excess EDAC and Sulfo-NHS. The solution was further dialyzed using a 3.5 kDa molecular weight cutoff dialysis membrane for 2 days to eliminate the free amino-phalloidin, and the Milli-Q water after each run of dialysis was collected and concentrated for HPLC analysis. HCPE-phalloidin was finally collected after freeze-drying.

Cellular Uptake Study of HCPE-Phalloidin and HCPE-COOH. Hela cells (2×10^4 cells/mL) were seeded into 96-well black plates (Costar, IL, USA) and incubated for 48 h to evaluate the cellular uptake processes. Four groups of cells were incubated with HCPE-phalloidin in FBS-free DMEM for 2 h at (A) 37 °C, (B) 4 °C, (C) 37 °C with pretreatment of sucrose, and (D) 37 °C with pretreatment of genistein, respectively. Six wells were used for each group. The cells incubated with (A) HCPE-phalloidin at 37 °C without inhibitor pretreatment was used as the control. To study the effect of incubation temperature on cellular uptake, we incubated the cells with (B) 1 μg/mL HCPE-phalloidin nanosphere solution for 2 h at 4 °C. To study the

Scheme 1. Synthetic Entry to HCPE-Phalloidin[a]

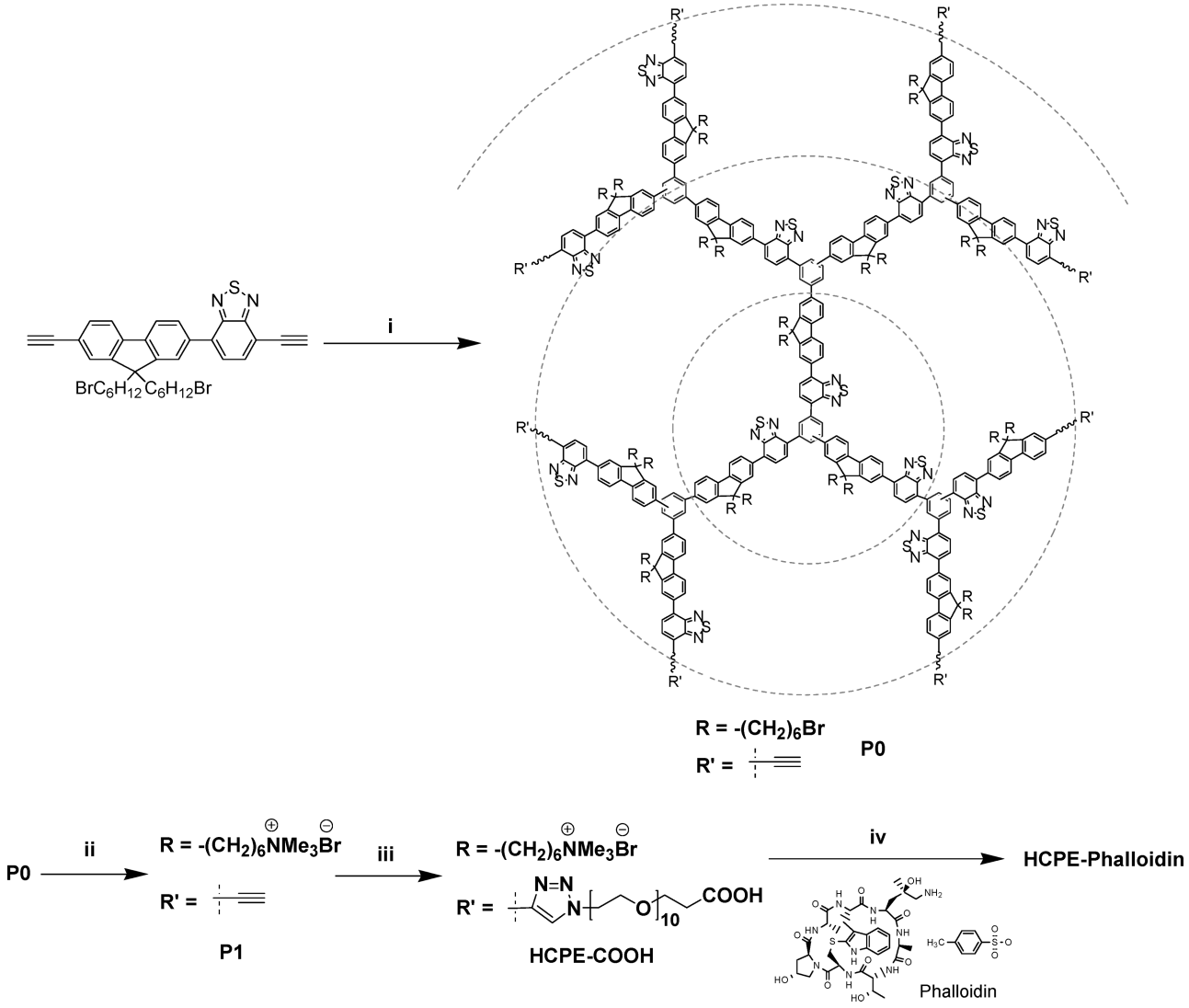

[a] Conditions and reagents: (i) toluene, $CpCo(CO)_2$, 65 °C, 8 h; (ii) THF/methanol, TMA, 24 h; (iii) DMF, PMDETA/CuBr, 65 °C, 24 h; (iv) borate buffer, EDAC/sulfo-NHS, RT, 3 h.

effect of different inhibitors on specific endocytosis processes, (C) fresh FBS-free DMEM medium supplemented with 4% w/v sucrose or (D) 0.2 mM genistein were added into each sample well and the cells were preincubated for 1 h at 37 °C. The medium was then removed and HCPE-phalloidin in FBS-free DMEM (1 μg/mL) was subsequently added into each sample well and incubated for 2 h at 37 °C. After incubation, the (A) control and (B−D) sample wells were washed twice with 50 μL 1× PBS buffer to remove traces of nanospheres. DMEM medium (100 μL, FBS free) was then added to each well, which was followed by addition of 50 μL of 0.5% Triton X-100 in 0.2 N NaOH to lyse the cells. The fluorescence intensity of HCPE-phalloidin nanospheres at 586 nm in each well was then measured by microplate reader (Genios Tecan) with excitation wavelength of 405 nm. The relative cellular uptake efficiency under different conditions was expressed as the ratio of the fluorescence in the corresponding sample wells to that of the control wells. The study of cellular uptake of HCPE-COOH was carried out following the same procedures.

Cytotoxicity of HCPE-COOH. Methylthiazolyldiphenyl-tetrazolium (MTT) assays were performed to assess the metabolic activity of Hela cells. Cells were seeded in 96-well plates (Costar, IL, USA) at an intensity of 2×10^4 cells/mL. After 48 h incubation, the old medium was replaced by the HCPE-COOH solution in medium at different HCPE-COOH concentrations, and the cells were then incubated for 12, 24, and 48 h, respectively. After the designated time intervals, the wells were washed twice with 1× PBS buffer and 100 μL of freshly prepared MTT (0.5 mg/mL) solution in culture medium was added into each well. The MTT medium solution was carefully removed after 3 h incubation in the incubator. DMSO (100 μL) was then added into each well and the plate was gently shaken for 10 min at room temperature to dissolve all the precipitates formed. The absorbance of MTT at 570 nm was monitored by the microplate reader. Cell viability was expressed by the ratio of absorbance of the cells incubated with nanosphere solution to that of the cells incubated with culture medium only.

F-Actin Labeling in Living Hela Cells. Hela cells were cultured in the confocal imaging chamber (LAB-TEK, Chambered Coverglass System) at 37 °C. After 80% confluence, the medium was removed and the adherent cells were washed twice with 1× PBS buffer. The HCPE-phalloidin in FBS free DMEM medium (1 μg/mL) was then added to

dx.doi.org/10.1021/cm103557h |*Chem. Mater.* 2011, 23, 2113–2119

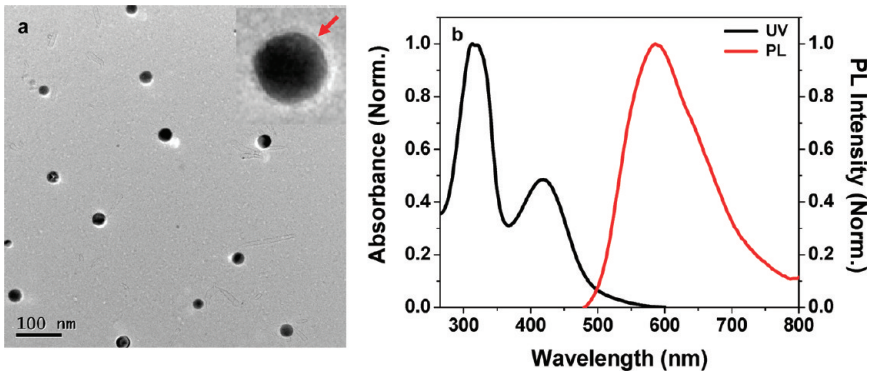

Figure 1. (a) High-resolution TEM image of HCPE-phalloidin nanospheres. (b) UV−vis absorption and PL spectra of HCPE-phalloidin in water (λ_{ex} = 419 nm).

the chambers. After incubation for 2 h, the cells were washed three times with 1× PBS buffer to eliminate the excess HCPE-phalloidin and imaged by confocal laser scanning microscope (CLSM, Zeiss LSM 410, Jena, Germany) with imaging software (Fluoview FV1000). HCPE-COOH for living cell imaging was also carried out following the same procedure. Hela cells cultured with Alexa Fluor 488-phalloidin in DMEM medium (0.1 μM, FBS free) for 2 h were also imaged.

F-Actin Labeling in Fixed and Permeabilized Hela Cells. Hela cells were cultured in the confocal imaging chamber (LAB-TEK, Chambered Coverglass System) at 37 °C. After 80% confluence, the medium was removed and the adherent cells were washed twice with 1× PBS buffer. The cells were fixed with 3.7% paraformaldehyde for 10 min at 37 °C and permeabilized with 0.1% triton X-100 for 5 min at room temperature. The fixed and permeabilized cells were further blocked by 1% BSA in 1× PBS buffer for 30 min and washed three times with 1× PBS buffer. The cells were then incubated with Alexa Fluor 488-phalloidin in 1× PBS buffer for 30 min at room temperature, respectively. After the cells were washed with 1× PBS buffer, imaging was carried out on confocal laser scanning microscope (CLSM, Zeiss LSM 410, Jena, Germany) with imaging software (Fluoview FV1000).

Colocalization of HCPE-Phalloidin and Alexa Fluor 594-Phalloidin in Hela Cell. Hela cells were cultured in the confocal imaging chamber (LAB-TEK, Chambered Coverglass System) at 37 °C. After 80% confluence, the medium was removed and the adherent cells were washed twice with 1× PBS buffer. The HCPE-phalloidin in FBS-free DMEM medium (1 μg/mL) was then added to the chambers. After incubation for 2 h, the cells were washed three times with 1× PBS buffer to eliminate the excess HCPE-phalloidin. The cells were then fixed using ethanol for 10 min at 37 °C. After washing for three times, the cells were incubated with Alexa Fluor 594-phalloidin in 1× PBS buffer (0.1 μM) for 40 min at room temperature. After washing with 1× PBS buffer, imaging was carried out on confocal laser scanning microscope (CLSM, Zeiss LSM 410, Jena, Germany) with imaging software (Fluoview FV1000). The fluorescence of HCPE-phalloidin was collected with a 490−560 nm band-pass filter upon 405 nm excitation (1.25 mW laser power) and that of Alexa Fluor 594-phalloidin was collected with a 565−655 nm band-pass filter upon 543 nm excitation (1 mW laser power). Under these experimental conditions, the fluorescence of HCPE-phalloidin is not detectable with the 565−655 nm band-pass filter and that of Alexa Fluor 594-phalloidin can not be detected in the 490−560 nm range.

Photostability Studies. The confocal samples of Hela cells incubated with HCPE-phalloidin or stained with Alexa Fluor 488-phalloidin were prepared according to previously described procedures. The CLSM images of each sample were recorded at 1 min interval under continuous laser scanning at excitation wavelength of 405 or 488 nm for HCPE-phalloidin and 488 nm for Alexa Fluor 488-phalloidin (1 mW for 405 nm laser and 1.25 mW for 488 nm laser). The fluorescence intensity of each image was analyzed by ImageJ software. The photostability of HCPE-phalloidin and Alexa Fluor 488-phalloidin was expressed by the ratio of fluorescence intensity of each sample after excitation for a designated time interval to its initial value as a function of exposure time.

RESULTS AND DISCUSSION

The neutral hyperbranched conjugated polymer (**P0**) was synthesized by alkyne polycyclotrimerization,[51] from 4-(9,9′-bis(6-bromohexyl)-7-ethynylfluorenyl)-7-ethynylbenzothiadiazole in 65% yield (see Scheme 1). From the ^{1}H NMR spectrum (see Figure S1a in the Supporting Information), the number average molecular weight of **P0** was estimated to be ∼16 000. Subsequent treatment of **P0** with trimethylamine (TMA) in tetrahydrofuran (THF)/methanol yielded water-soluble **P1** in 95% yield with ∼93% quaternization degree. The attachment of N_3−PEG-COOH to **P1** was achieved through click reaction, which was carried out at 65 °C for 24 h under nitrogen in dimethylformamide (DMF) using *N,N,N′,N″,N″*-pentamethyldiethylenetriamine (PMDETA) and CuBr as the catalyst. The obtained HCPE-COOH was purified by microfiltration and precipitation, which was followed by dialysis against Milli-Q water for 5 days and freeze-drying. The ^{1}H NMR spectrum (see Figure S1b in the Supporting Information) of HCPE-COOH reveals that the residual alkynes are almost completely converted to triazole groups (∼14 PEG-COOH/**P1**). The HCPE-COOH was subsequently functionalized with amino-phalloidin through *N*-(3-dimethylaminopropyl)-*N′*-ethylcarbodiimide hydrochloride (EDAC) mediated coupling reaction in the presence of *N*-hydroxysulfosuccinimide sodium salt (Sulfo-NHS) at room temperature for 3 h. The final conjugate (HCPE-phalloidin) was purified by dialysis against Milli-Q water for 3 days, followed by freeze-drying. High-performance liquid chromatography (HPLC) was employed to quantify the number of phalloidin molecules conjugated to HCPE-COOH, suggesting that on average each HCPE-phalloidin conjugate has ∼5 phalloidin molecules. Detailed analysis of the ^{1}H NMR spectra for **P0** and **HCPE-COOH** is described in the Supporting Information.

High-resolution transmission electron microscopy (HR-TEM) was employed to study the morphology of the HCPE-phalloidin in solid state. As shown in Figure 1a, HCPE-phalloidin forms spherical nanospheres with a core−shell structure, which consists of a dark interior (electron-rich conjugated segments) and a gray exterior (saturated PEG segments and phalloidin). Statistical calculation from HR-TEM images indicates that the

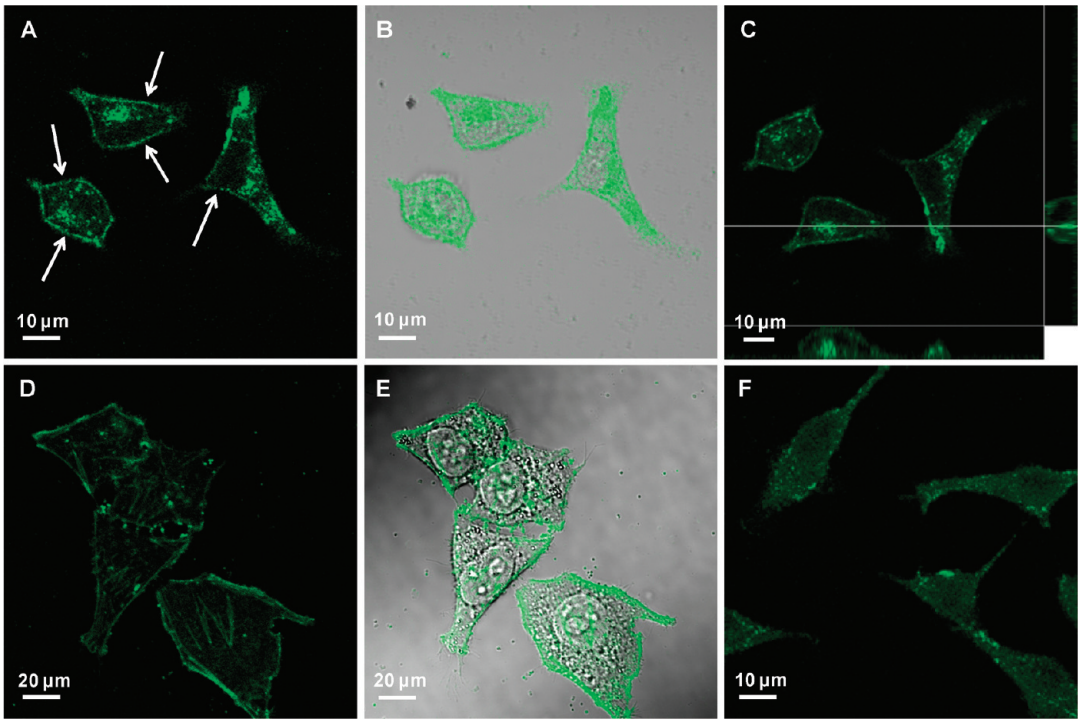

Figure 2. (A) Confocal image, (B) fluorescence/transmission overlapped image, and (C) 3D sectional confocal image of the Hela cells after incubation with 1 μg/mL HCPE-phalloidin in culture medium for 2 h at 37 °C (λ_{ex} = 405 nm, 1 mW laser power). (D) Confocal image and (E) fluorescence/transmission overlapped image of the fixed and permeabilized Hela cells stained by Alexa Fluor 488-phalloidin (λ_{ex} = 488 nm, 1.25 mW laser power). (F) Confocal image of the Hela cells after incubation with 1 μg/mL HCPE-COOH for 2 h at 37 °C (λ_{ex} = 405 nm, 1 mW laser power).

average diameter of HCPE-phalloidin is 26 ± 2 nm, which is slightly smaller than that determined from laser light scattering (LLS) with an average hydrodiameter of 32 ± 3.0 nm in aqueous solution, due to shrinkage of the polymeric nanospheres during drying process.[26] The hydrodiameter of HCPE-COOH is also measured to be 32 ± 3.5 nm, suggesting that conjugation of phalloidin molecule has negligible effect on the nanosphere size. Figure 1b shows the UV−vis absorption and photoluminescence (PL) spectra of HCPE-phalloidin in water. The absorption spectrum has two peaks at 317 and 419 nm, and the PL spectrum has a maximum of 586 nm, which match the confocal laser scanning microscope (CLSM) with 405 nm excitation and 520 nm long-pass barrier filter for signal collection.

The ability of HCPE-phalloidin nanospheres to label F-actin in living Hela cells was investigated by CLSM, and the corresponding images are shown in Figure 2. The experimental conditions are set so that no autofluorescence from cells is detectable (see Figure S2 in the Supporting Information). Under the same laser and filter setup, the confocal and fluorescence/transmission overlapped images of Hela cells after incubation with 1 μg/mL of HCPE-phalloidin for 2 h at 37 °C were obtained and illustrated in images A and B in Figure 2, respectively. The images were taken by focusing on the bottom layer of cells to monitor F-actin distribution. It is obvious that the cell periphery is brighter than other region of the cells, which is similar to that for fixed and permeabilized Hela cells stained with commercial Alexa Fluor 488-phalloidin (Figure 2D, E). This result indicates specific interaction between HCPE-phalloidin and F-actin, which is concentrated more along the cell periphery than in the cytoplasm of Hela cells.[46−50] The 3D sectional CLSM image of the corresponding cells in Figure 2C further confirms that the

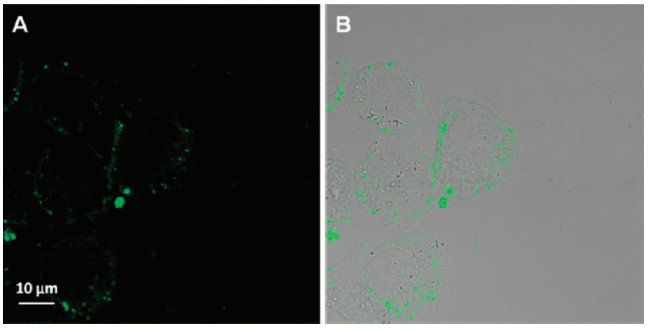

Figure 3. (A) Confocal image and (B) fluorescence/transmission overlapped image of living Hela cells after incubation with 0.1 μM Alexa Fluor 488-phalloidin in culture medium for 2 h at 37 °C (λ_{ex} = 488 nm, 1.25 mW laser power).

HCPE-phalloidin nanospheres are internalized into living Hela cells to label F-actin underneath the cell membrane.[52,53] The specificity of HCPE-phalloidin to F-actin was further investigated by using commercial Alexa Fluor 594-phalloidin to stain the fixed Hela cells that were first incubated with HCPE-phalloidin for 2 h at 37 °C (see Figure S3 in the Supporting Information). The yellow fluorescence along the cell periphery in Figure S3C indicates that fluorescence from HCPE-phalloidin and Alexa Fluor 594-phalloidin is colocalized in good agreement.

The CLSM image shown in Figure 2A also indicates that the HCPE-phalloidin nanospheres have better performance in living cell actin imaging as compared to that for various nanocarrier promoted QD and organic fluorophore based phalloidin conjugates.[10,13,14,31] It is important to note that Alexa Fluor

dx.doi.org/10.1021/cm103557h |*Chem. Mater.* 2011, 23, 2113–2119

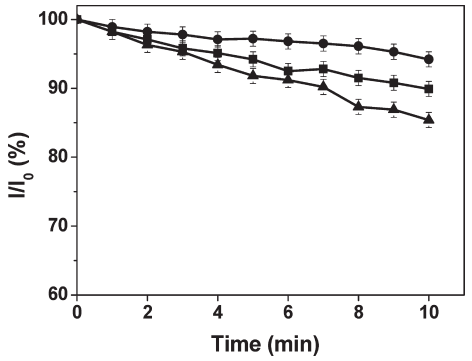

Figure 4. Photostability comparison between HCPE-phalloidin upon continuous excitation at 488 nm (circles), 405 nm (squares), and Alexa Fluor 488-phalloidin upon continuous laser excitation at 488 nm (triangles) for 0 to 10 min (1 mW for 405 nm laser and 1.25 mW for 488 nm laser). I_0 is the initial fluorescence intensity and I is the fluorescence intensity of the corresponding sample after continuous scanning for designated time intervals.

488-phalloidin is not able to clearly label F-actin upon direct incubation with living Hela cells as organic chromophore phalloidin conjugates have low living cell membrane permeability (Figure 3).[6−10] In addition, when HCPE-COOH is used for direct incubation with living Hela cells, the nanospheres are found to uniformly distributed in cell cytoplasm (Figure 2F), which clearly indicates the importance of phalloidin-HCPE conjugation on specific F-actin labeling.

The uptake mechanism of HCPE-phalloidin was studied by comparing the fluorescence intensity from Hela cells after incubation with the same concentration of HCPE-phalloidin for 2 h under different conditions,[35,54] using the cells incubated with HCPE-phalloidin at 37 °C as the control. Quantitative cellular uptake studies reveal that the uptake of HCPE-phalloidin by Hela cells at 4 °C is significantly reduced to 13% of that at 37 °C, indicating that the nanospheres are internalized into Hela cells through an energy-dependent pathway.[35,54] On the other hand, the uptake of HCPE-phalloidin at 37 °C is equivalent to 99% and 96% of the control when Hela cells are pretreated with sucrose and genistein, the specific endocytic process inhibitors for clathrin- and caveolae-mediated endocytosis.[55,56] These results suggest that HCPE-phalloidin nanospheres are internalized through a clathrin- and caveolae-independent energy-dependent pathway.[54,57] Similarly, the uptake of HCPE-COOH by Hela cells at 4 °C is 11% of that at 37 °C, whereas the uptake after treatment with sucrose and genistein is 101 and 98% of the control, respectively. These results suggest that the attachment of phalloidin molecules does not alter the internalization pathway of the HCPE nanospheres into Hela cells. Moreover, the metabolic viability of Hela cells remains above 94% after culture with 0.1 mg/mL HCPE-COOH for 48 h, indicating very low cytotoxicity of the nanospheres (Figure S4 in the Supporting Information). Considering their good living cell permeability and low cytotoxicity, various functionalized HCPE nanospheres with recognition groups could be designed for specific target imaging in living cells.

The photostability of the HCPE-phalloidin in Hela cells was also studied under continuous laser scanning upon excitation at 405 and 488 nm for HCPE-phalloidin and 488 nm for Alexa Fluor 488-phalloidin, respectively. As shown in Figure 4, HCPE-phalloidin shows ~6% and ~11% decrease of fluorescence intensity under continuous laser excitation at 488 and 405 nm for 10 min, respectively, which is obviously less as compared to that for Alexa Fluor 488-phalloidin under the same condition. As Alexa Fluor is well-known for its high photostability,[6] this study indicates that HCPE-phalloidin is a promising fluorescent probe for long-term F-actin imaging in living cells.

CONCLUSION

In conclusion, we demonstrate F-actin cytoskeleton imaging in living Hela cells using phalloidin-modified HCPE nanospheres as the fluorescent probe. The probe design takes advantage of unique hyperbranched core−shell molecular structure that facilitates cellular uptake and the phalloidin molecules that specifically bind to F-actin. Visualization of F-actin is realized through direct incubation of the cells with HCPE-phalloidin for 2 h at 37 °C, and the nanospheres are internalized through clathrin- and caveolae-independent energy-dependent pathway, which eliminates the needs for specific instruments or sophisticated techniques to induce cellular internalization. As the size and fluorescent properties of HCPEs could be fine-tuned through conjugated core design and the targeting ability of HCPEs can also be desirably modified through conjugation with diverse biorecognition moieties, this study provides a novel molecular design concept for CPEs to meet the needs for complicated biological imaging and detection. The first demonstration of CPEs for intracellular target detection will inspire great enthusiasm in the development of novel CPE-based probes for subcellular protein imaging and tracking in living cells.

ASSOCIATED CONTENT

Supporting Information. Characterization of HCPE-COOH and HCPE nanospheres. ^{1}H NMR spectra of **P0** and HCPE-COOH, confocal image of Hela cells without HCPE-phalloidin incubation, colocalization of HCPE-phalloidin and Alexa Fluor 594-phalloidin in Hela cells, and metabolic viability of Hela cells upon treatment with HCPE-COOH nanospheres. This material is available free of charge via the Internet at http://pubs.acs.org.

AUTHOR INFORMATION

Corresponding Author
*E-mail: cheliub@nus.edu.sg.

ACKNOWLEDGMENT

The authors are grateful to the National Research Foundation (R279-000-323-281), National University of Singapore (R279-000-301-646), Ministry of Education (R279-000-255-112), and Temasek Defence Systems Institute (R279-000-301-232) for financial support. The authors also thank Dr. J. B. Shi for support in polymerization, H. Yin for support in cell culture, Y. H. Tee for support in actin staining and S. Y. Lee for support in CLSM imaging experiments. K. Li thanks NUS for support via a research fellowship.

REFERENCES

(1) Jordan, M. A.; Wilson, L. *Cur. Opin. Cell Biol.* **1998**, *10*, 123.
(2) Stephens, D. J.; Allan, V. J. *Science* **2003**, *300*, 82.
(3) Cingolani, A. L.; Yukiko, G. *Nat. Rev. Neurosci.* **2008**, *9*, 344.
(4) Theriot, J. A.; Mitchison, T. J. *Nature* **1991**, *352*, 126.

(5) Kaksonen, M.; Sun, Y.; Drubin, D. G. *Cell* **2003**, *115*, 475.
(6) Invitrogen, Probes for Actin. http://www.invitrogen.com/site/us/en/home/References/Molecular-Probes-The-Handbook/Probes-for-Cytoskeletal-Proteins/Probes-for-Actin.html.
(7) Taylor, D. L.; Wang, Y. L. *Nature* **1980**, *284*, 405.
(8) Wulf, E.; Deboben, A.; Bautz, F. A.; Faulstich, H.; Wieland, T. *Proc. Natl. Acad. Sci. U.S.A.* **1979**, *76*, 4498.
(9) Cooper, J. A. *J. Cell. Biol.* **1987**, *105*, 1473.
(10) Barber, K.; Mala, R. R.; Lambert, M. P.; Qiu, R.; MacDonald, R. C.; Klein, W. L. *Neurosci. Lett.* **1996**, *207*, 17.
(11) Waterman-Storer, C. M.; Desai, A.; Bulinski, J. C.; Salmon, E. D. *Curr. Biol.* **1998**, *8*, 1227.
(12) Derfus, A. M.; Chan, W. C. W.; Bhatia, S. N. *Adv. Mater.* **2004**, *16*, 961.
(13) Yoo, J.; Kambara, T.; Gonda, K.; Higuchi, H. *Exp. Cell Res.* **2008**, *314*, 3563.
(14) Kim, B. Y. S.; Jiang, W.; Oreopoulos, J.; Yip, C. M.; Rutka, J. T.; Chan, W. C. W. *Nano Lett.* **2008**, *8*, 3887.
(15) Choidas, A.; Jungbluth, A.; Sechi, A.; Murphy, J.; Ullrich, A.; Marriott, G. *Eur. J. Cell Biol.* **1998**, *77*, 81.
(16) Riedl, J.; Crevenna, A. H.; Kessenbrock, K.; Yu, J. H.; Neukirchen, D.; Bista, M.; Bradke, F.; Jenne, D.; Holak, T. A.; Werb, Z.; Sixt, M.; Wedlich-Söldner, R. *Nat. Methods* **2008**, *5*, 605.
(17) He, Y.; Kang, Z. H.; Li, Q. S.; Tsang, C. H. A.; Fan, C. H.; Lee, S. T. *Angew. Chem., Int. Ed.* **2009**, *48*, 128.
(18) Liu, B.; Bazan, G. C. *Chem. Mater.* **2004**, *16*, 4467.
(19) Duarte, A.; Pu, K. Y.; Liu, B.; Bazan, G. C. *Chem. Mater.* **2011**, *23*, 501.
(20) McQuade, D. T.; Pullen, A. E.; Swager, T. M. *Chem. Rev.* **2000**, *100*, 2537.
(21) Thomas, S. W., III; Joly, G. D.; Swager, T. M. *Chem. Rev.* **2007**, *107*, 1339.
(22) Ho, H. A.; Najari, A.; Leclerc, M. *Acc. Chem. Res.* **2008**, *41*, 168.
(23) Sigurdson, C. J.; Nilsson, K. P. R.; Hornemann, S.; Manco, G.; Polymenidou, M.; Schwarz, P.; Leclerc, M.; Hammarström, P.; Wüthrich, K.; Aguzzi, A. *Nat. Methods* **2007**, *4*, 1023.
(24) McRae, R. L.; Phillips, R. L.; Kim, I. B.; Bunz, U. H. F.; Fahrni, C. J. *J. Am. Chem. Soc.* **2008**, *130*, 7851.
(25) Rahim, N. A. A.; McDaniel, W.; Bardon, K.; Srinivasan, S.; Vickerman, V.; So, P. T. C.; Moon, J. H. *Adv. Mater.* **2009**, *21*, 3492.
(26) Pu, K. Y.; Li, K.; Shi, J.; Liu, B. *Chem. Mater.* **2009**, *21*, 3816.
(27) Feng, X. L.; Tang, Y. L.; Duan, X. R.; Liu, L. B.; Wang, S. *J. Mater. Chem.* **2010**, *20*, 1312.
(28) Pu, K. Y.; Li, K.; Liu, B. *Adv. Mater.* **2010**, *22*, 643.
(29) Pu, K. Y.; Li, K.; Zhang, X. H.; Liu, B. *Adv. Mater.* **2010**, *22*, 4186.
(30) Smith, A. M.; Duan, H.; Mohs, A. M.; Nie, S. M. *Adv. Drug Delivery Rev.* **2008**, *60*, 1226.
(31) Adurkar, U. S.; Agrawal, A.; Nie, S. M. *Proc. SPIE* **2005**, *5699*, 189.
(32) Pu, K. Y.; Li, K.; Liu, B. *Adv. Funct. Mater.* **2010**, *20*, 2770.
(33) Pu, K. Y.; Li, K.; Liu, B. *Chem. Mater.* **2010**, *22*, 6736.
(34) Chithrani, B. D.; Ghazani, A. A.; Chan, W. C. W. *Nano Lett.* **2006**, *6*, 662.
(35) Lai, S. K.; Hida, K.; Man, S. T.; Chen, C.; Machamer, C.; Schroer, T. A.; Hanes, J. *Biomaterials* **2007**, *28*, 2876.
(36) Wang, Z. J.; Tiruppathi, C.; Minshall, R. D.; Malik, A. B. *ACS Nano* **2009**, *3*, 4110.
(37) Zeng, F.; Zimmerman, S. C. *Chem. Rev.* **1997**, *97*, 1681.
(38) Inoue, K. *Prog. Polym. Sci.* **2000**, *25*, 453.
(39) Tian, Z.; Yu, J.; Wu, C.; Szymanski, C.; McNeill, J. *Nanoscale* **2010**, *2*, 1999.
(40) Xu, K. T.; Peng, H.; Sun, Q. H.; Dong, Y. P.; Salhi, F.; Luo, J. D.; Chen, J. W.; Huang, Y.; Zhang, D. Z.; Xu, Z. D.; Tang, B. Z. *Macromolecules* **2002**, *35*, 5821.
(41) Chen, J. W.; Peng, H.; W. Law, C. C.; Dong, Y. P.; Lam, J. W. Y.; Williams, I. D.; Tang, B. Z. *Macromolecules* **2003**, *36*, 4319.
(42) Tolosa, J.; Kub, C.; Bunz, U. H. F. *Angew. Chem., Int. Ed.* **2009**, *48*, 4610.
(43) Yoo, H.; Juliano, R. L. *Nucl. Acid Res.* **2000**, *28*, 4225.
(44) Faulstich, H. *Crit. Rev. Biochem.* **1978**, *5*, 185.
(45) Vandekerckhove, J.; Deboben, A.; Nassal, M.; Wieland, T. *EMBO J.* **1985**, *4*, 2815.
(46) Wu, X.; Kocher, B.; Wei, Q.; Hammer, J. A., III. *Cell Motil. Cytoskel.* **1998**, *40*, 286.
(47) Rodgers, W.; Zavzavadjian, J. *Exp. Cell Res.* **2001**, *267*, 173.
(48) Paul, C.; Manero, F.; Gonin, S.; Kretz-Remy, C.; Virot, S.; Arrigo, A. P. *Mol. Cell. Biol.* **2002**, *22*, 816.
(49) Szczepanowska, J.; Korn, E. D.; Brzeska, H. *Cell Motil. Cytoskel.* **2006**, *63*, 356.
(50) Paul, C.; Simon, S.; Gibert, B.; Virot, S.; Manero, F.; Arrigo, A. P. *Exp. Cell Res.* **2010**, *316*, 1535.
(51) Liu, J.; Lam, J. W. Y.; Tang, B. Z. *Chem. Rev.* **2009**, *109*, 5799.
(52) Mabuchi, I. *Int. Rev. Cytol.* **1986**, *101*, 175.
(53) Kamasaki, T.; Osumi, M.; Mabuchi, I. *J. Cell Biol.* **2007**, *178*, 765.
(54) Khalil, I. A.; Kogure, K.; Akita, H.; Harashima, H. *Pharmacol. Rev.* **2006**, *58*, 32.
(55) Heuser, J. E.; Anderson, R. G. *J. Cell Biol.* **1989**, *108*, 389.
(56) Le, P. U.; Nabi, I. R. *J. Cell Sci.* **2003**, *116*, 1059.
(57) Conner, S. D.; Schmid, S. L. *Nature* **2003**, *422*, 37.